

# Preparation and characterization of CuI nanorods using $\text{Cu}(\text{dmg})_2$ as precursor via water-in-oil (w/o) microemulsions

Xue-Liang Li <sup>a,\*</sup>, Xiao-Yun Zhu <sup>a</sup>, Ti-Lan Duan <sup>a</sup>, Yi-Tai Qian <sup>b</sup>

<sup>a</sup> School of Chemical Engineering, Hefei University of Technology, Hefei 230009, People's Republic of China

<sup>b</sup> Hefei National Laboratory for Physical Sciences at Microscale and Department of Chemistry, University of Science and Technology of China, Hefei, Anhui 230026, People's Republic of China

Received 22 August 2005; received in revised form 20 January 2006; accepted 15 April 2006 by B.-F. Zhu

Available online 6 May 2006

## Abstract

CuI nanorods have been firstly prepared by water-in-oil microemulsions using  $\text{Cu}(\text{dmg})_2$  as precursor at low temperature as low as 70 °C. X-ray diffraction (XRD) and transmission electron microscopy (TEM) measurements show that the CuI nanorods are pure  $\gamma$ -phase crystals with diameters ranging from 50 to 80 nm and lengths up to 500 nm. UV–vis spectrum reveals that the nanorods exhibit a blue shift and possess of wider band gap energy. Electrochemical impedance spectroscopy (EIS) reveals the nanorods own larger grain boundary resistance. Results of comparative experiments indicate that the rod-like structure of  $\text{Cu}(\text{dmg})_2$  crystals leads the CuI crystals growing in one direction especially and the reverse microemulsion system plays a crucial role in making products symmetrical and uniform.

© 2006 Elsevier Ltd. All rights reserved.

PACS: 73.61.Tm; 73.40.−c; 74.25.Gz; 81.05.Dz; 81.20.Ka

Keywords: A. Nanostructures; B. Crystal growth; C. Grain boundaries; D. Optical properties

## 1. Introduction

Cuprous iodide is water insoluble solid with three crystalline phases  $\alpha$ ,  $\beta$  and  $\gamma$  [1,2].  $\gamma$ -CuI is a p-type semiconductor with direct band gap [3,4]. Due to its electrical properties, it is used as a holecollecting agent in dye sensitized solid-state cell [5], superconductors [6], catalysts for synthesis of organic compound [7], and effective adsorbents for separating carbon monoxide from gas mixtures [8].

There are several methods for preparing CuI, such as electrodeposition [9], pulsed laser deposition [10], liquid phase reaction [11] and vacuum evaporation [12]. To the best of our knowledge, there have been few reports on preparations of CuI nanoparticles [13,14], and no report on CuI nanorods. In this paper, we firstly synthesized CuI nanorods by  $\text{Cu}(\text{dmg})_2$  and KI in a reverse microemulsion system at 70 °C. The products were characterized by XRD, TEM, UV and EIS. Results showed different optical and electrical properties of CuI nanorods in

comparison with bulk materials, which may be very useful for many device applications.

## 2. Experimental

All reagents were of analytical grade and used without further purification.

First, 0.464 g of Dimethylglyoxime (dmGH) and 0.400 g of  $\text{Cu}(\text{Ac})_2 \cdot \text{H}_2\text{O}$  were added into 50 ml of absolute ethanol in sequence, which was stirred at the room temperature for 30 min to get brown precipitates  $\text{Cu}(\text{dmg})_2$ . Then the collected precipitates were dried in air at 60 °C and dispersed in 10 ml of distilled water. Secondly, 30 ml of cyclohexane, 1 ml of *n*-Amyl alcohol, 1.511 g of SDS and 2 ml of  $\text{Cu}(\text{dmg})_2$  suspension were mixed and stirred vigorously to form microemulsion I. And microemulsion II was made at the same condition except that  $\text{Cu}(\text{dmg})_2$  suspension was replaced by 0.4 mol l<sup>−1</sup> KI aqueous solution. Thirdly, Microemulsion I was added to Microemulsion II with slow stirring and the mixture was stirred for 2 h, which was manipulated in water bath at 70 °C. Finally, the product was centrifuged, washed and vacuum dried in sequence for the following characterizations.

The samples were characterized by powder X-ray diffraction (XRD) on a D/Max-rB X-ray diffractometer with

\* Corresponding author.

E-mail address: [xueliangli2005@163.com](mailto:xueliangli2005@163.com) (X.-L. Li).

monochromatized Cu K $\alpha$  ( $\lambda=1.5406 \text{ \AA}$ ) incident radiation. XRD patterns were recorded from 20 to 55° ( $2\theta$ ) with a scanning rate of 6°/min. The morphologies of the samples were analyzed by TEM on an H-800 transmission electron microscope operated at 200 kV. Optical absorption spectrum was recorded on a Shimadzu UV-2401PC UV–vis recording spectrophotometer. Impedances were measured on CHI660B electrochemical workstation in the frequency range of 100 Hz to 10 mHz at the init  $E -0.5 \text{ V}$  (vs. Hg/HgO (6 M KOH) electrode).

In the process of EIS measurement, electrodes were prepared by mechanically pressing (200 kg/cm<sup>2</sup>) the well-mixed CuI powders of carbon black and PTFE powders on titanium flakes (the area of the cathode 10 mm  $\times$  10 mm). The composition of the electrodes is CuI, carbon and polytetrafluoroethylene (PTFE) with weight ratio of 8.5:1:0.5. A 6 M solution of KOH in distilled water was used as the electrolyte. A platinum electrode and an Hg/HgO (6 M KOH) electrode were used as the counter electrode and reference electrode, respectively.

### 3. Results and discussion

The XRD pattern of the product is shown in Fig. 1. All diffraction peaks in the XRD pattern can be perfectly indexed to pure  $\gamma$ -phase CuI (JCPDS, 06-0246). No impurity was detected, indicating that the as-synthesized product was of high purity. The average crystalline size of the product can be estimated by Scherrer equation

$$D = (K\lambda)/\beta \cos \theta$$

where  $D$  is the mean diameter of the nano-particles,  $K$  is a constant (0.89),  $\lambda$  is the X-ray wavelength (0.15406 nm in the present case),  $\beta$  is the corrected X-ray diffraction broadening ( $\beta=B-b$ ,  $B$  stands for full width at half maximum and  $b$  is the instrumental line broadening), and  $\theta$  is the Bragg angle of the X-ray diffraction peak. Calculation made on the strongest peak at  $2\theta=25.40^\circ$  is 79.1 nm. Actually, the size obtained from XRD pattern broadening is the mean size of single crystal in the sample. However, the size observed by TEM is the size of the single particles and the single particles maybe consisted of several single crystals (in the case that some rods are not single

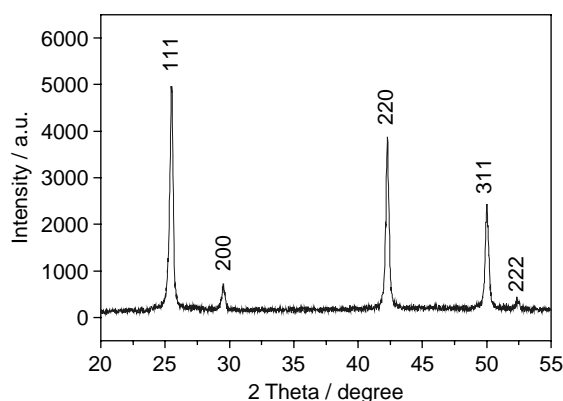


Fig. 1. XRD pattern of the as-prepared CuI.

crystal). So the calculation according XRD pattern is coincident with the value measured by TEM. The little disaccord can be attributed to the following reason.

The morphologies of the as-prepared CuI and Cu(dmg)<sub>2</sub> crystals were studied by TEM. Fig. 2(a–c) shows that the CuI crystals are nanorods with diameters ranging from 50 to 80 nm and lengths up to 500 nm, and this morphology has not been reported in other papers. The ED pattern in Fig. 2(b) shows the nanorod is single crystal, which indicates that as-obtained CuI nanorods are mainly single crystals. Compared to the JCPDS card, the (220) peak is stronger, revealing the [220] oriented growth of the CuI nanorods. This new morphology of CuI might be mainly attributed to the morphology of the precursor Cu(dmg)<sub>2</sub>. In Fig. 2(d), we can find that the Cu(dmg)<sub>2</sub> crystals exhibit rod-like structure and this structure might lead the CuI crystals growing in one direction, especially. To prove this deduce, CuI prepared by Cu(Ac)<sub>2</sub> in the same conditions was studied by TEM. In Fig. 3(a), the typical morphology of the sample is triangle flake and no one-dimensional morphology can be observed.

The role of reverse microemulsion system can be seen clearly from two images of Fig. 3. The sample in Fig. 3(b) was synthesized just in aqueous solution without microemulsions. The image shows large agglomerates and no single crystal can be seen apart. The sample in Fig. 3(a) was synthesized in microemulsion. Compared to Fig. 3(b), most of the crystals in Fig. 3(a) are thin triangle flakes. So the reverse microemulsion

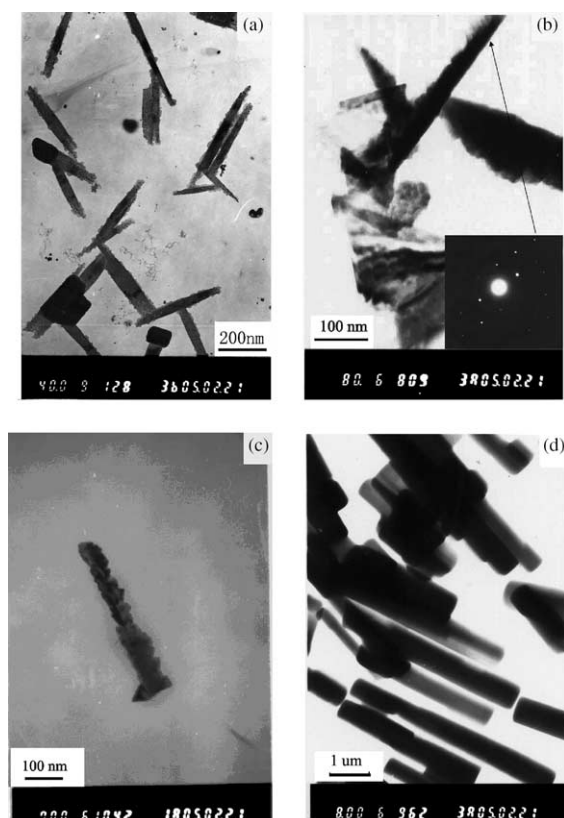


Fig. 2. (a)–(c): TEM images of the CuI nanorods prepared from Cu(dmg)<sub>2</sub> and its ED pattern, which shows single crystal; (d) TEM image of the Cu(dmg)<sub>2</sub> rods.

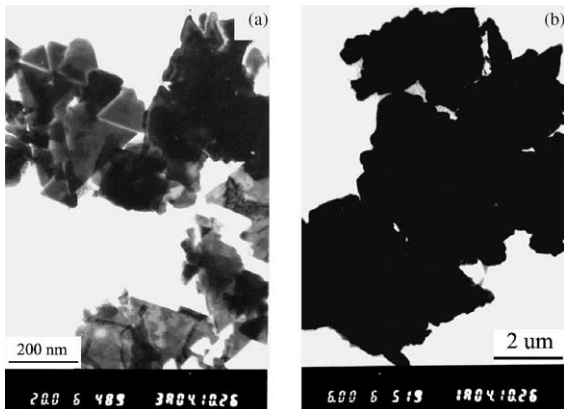


Fig. 3. TEM images of the CuI prepared from  $\text{Cu}(\text{Ac})_2$  (a) in microemulsions; (b) without microemulsions.

system plays a crucial role in making the as-prepared crystals dispersed.

Fig. 4 shows the optical absorption spectrum of as-synthesized CuI nanorods. Three strong absorption peaks centered at 220, 278 and 412 nm are shown in the UV spectrum, which is attributed to band gap absorptions in CuI [3,4]. The optical band gap  $E_g$  can be determined by the following equation

$$(Ah\nu)^n = B(h\nu - E_g)$$

where  $h\nu$  is the photo energy,  $A$  is absorbency,  $B$  is a constant relative to the material,  $n$  is either 2 for direct interband gap or 1/2 for indirect interband gap transitions [15]. The  $(Ah\nu)^2 - h\nu$  curve for the sample is shown in the inset of Fig. 4, which exhibits the as-obtained CuI nanorods have direct band gap. Calculated by the extrapolation of above equation, the band gaps are 2.37, 3.22 and 4.88 eV, respectively. These values are a little higher than the previously reported values of the band gap energies of CuI by B. Bouhafs et al. [3], which causes the blue shifts.

The impedance spectra ( $Z''$  plotted against  $Z'$ ) for as-prepared nano-CuI and agglomerate CuI are shown in Fig. 5. In the high-frequency region, the impedance of the

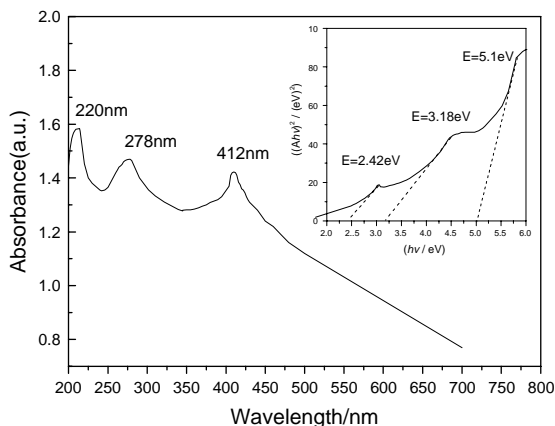


Fig. 4. Optical absorption spectrum and  $(Ah\nu)^2 - h\nu$  curve (inset) of as-synthesized CuI nanorods.

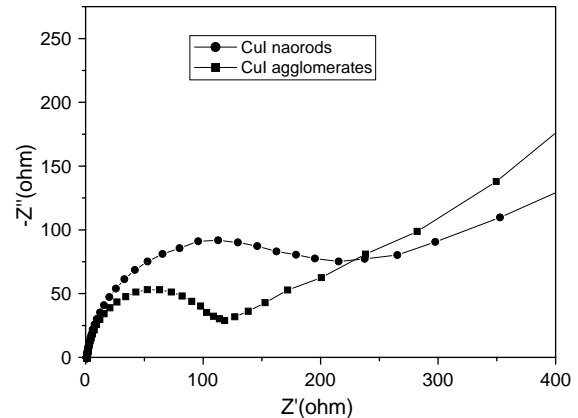


Fig. 5. Impedance spectra of CuI nanorods prepared as typical process in our paper and CuI agglomerates prepared from  $\text{Cu}(\text{Ac})_2$  without microemulsions.

semicircle is related to the reaction of the interface between solution and electrode. And the diameter of the arc indicates the resistance of electrode material. Because the electrodes are prepared in the same condition and with the same assistant materials (carbon, PTFE), so the major factor leading to the difference of the EIS measurement result is the CuI. Compared to the agglomerate CuI, the resistance value of nano-CuI is about twice, which is attributed to discontinuous grain boundaries and larger grain boundary resistance of the nanocrystalline [16,17]. In the low-frequency area, a clear linear part is observed, which is attributed to Warburg impedance caused by a semi-infinite to finite diffusion behavior.

#### 4. Conclusions

CuI nanorods with diameters ranging from 50 to 80 nm and lengths up to 500 nm have been firstly prepared by the reaction of  $\text{Cu}(\text{dmg})_2$  and KI at 70 °C in a reverse microemulsion system. X-ray diffraction, transmission electron microscopy, optical absorption spectrum and electrochemical impedance spectroscopy were used to characterize the samples. It shows that the rod-like-structure  $\text{Cu}(\text{dmg})_2$  as precursors can lead the CuI especially growing in one direction to form one-dimensional materials and the reverse microemulsion system plays a crucial role in making products symmetrical and uniform. Energy bands of the sample show blue shifts comparing with bulk materials, which are attributed to the quantum size confinement effect of the nanorods. Impedance spectrum indicates that the value of CuI nano-particles is larger than that of CuI agglomerates for the larger grain boundary resistance of nano-particles.

#### Acknowledgements

This paper was supported by Natural Science Foundation of Anhui Province of China (Grant No. 050440303). The authors wish to gratefully acknowledge Mr Shupeitang, Mr Anping

Liu and Mr Xiangying Chen for their cooperation and kind help.

## References

- [1] A. Chahid, R.L. Mcgreevy, *Physics*. B 234 (1997) 87.
- [2] W. Buhner, W. Halg, *Electrochim. Acta* 22 (1977) 701.
- [3] B. Bouhafis, H. Heireche, W. Sekkal, H. Aourag, M. Certier, *Phys. Lett. A* 240 (1998) 257.
- [4] W. Sekkal, A. Zaoui, *Phys. B* 315 (2002) 201.
- [5] K. Tennakone, G.R.R.A. Kumara, A.R. Kumarasinghe, K.U.G. Wijayantha, P.M. Sirmanne, *Semicond. Sci. Technol.* 10 (1995) 1689.
- [6] J. Bardeen, J. Less, *Common Met.* 62 (1978) 447.
- [7] A. Kelkar, M. Patil, V. Chaudhari. *Tetrahedron Lett.* 43 (2002) 7143.
- [8] L.N. Pribytkova, M.S. Erzhanova, *Khim. Prir. Soedin* 2 (1994) 212.
- [9] T. Takeda, K. Matsuaga, T. Uruga, M. Takakura, T. Fujiwara, *Tetrahedron Lett.* 38 (1997) 2879.
- [10] G. Zeni, J.V. Comasseto, *Tetrahedron Lett.* 40 (1997) 4619.
- [11] P.M. Sirimanne, M. Rusop, T. Shirata, T. Soga, T. Timbo, *Chem. Phys. Lett.* 66 (2002) 485.
- [12] K. Tennakone, G.R.R.A. Kumara, I.R.M. Kottedoda, V.P.S. Perera, G.M.L.P. Aponsu, K.G.U. Wijayantha, *Sol. Energy Mater.* 55 (1998) 283.
- [13] Y.J. Zhu, Y.T. Qian, Y.F. Cao, *Mater. Sci. Eng. B57* (1999) 247.
- [14] M. Yang, J.Z. Xu, S. Xu, J.J. Zhu, H.Y. Chen, *Inorg. Chem. Commun.* 7 (2004) 628.
- [15] A. Hagfeldt, M. Gratzel, *Chem. Rev.* 95 (1995) 49.
- [16] L. Ding, L.A. Wang, F.L. Zheng, *Physical Experiment of College* 9 (1996).
- [17] A. Chandra Bose, D. Kalpana, P. Thangadurai, S. Ramasamy, *J. Power Sources* 107 (2002) 138.